ELSEVIER

Journal of Alloys and Compounds 311 (2000) 153–158

Journal of ALLOYS AND COMPOUNDS

www.elsevier.com/locate/jallcom

X-ray diffraction study on the short-range structure of K_2O–TeO_2 glasses and melts

Yasuhiko Iwadate[a,*], Takeshi Mori[a], Takeo Hattori[a], Shin Nishiyama[a], Kazuko Fukushima[a], Norimasa Umesaki[b], Ryuichi Akagi[c], Katsumi Handa[d], Norikazu Ohtori[e], Tetsuya Nakazawa[f], Akira Iwamoto[f]

[a]*Department of Materials Technology, Faculty of Engineering, Chiba University, Yayoi-cho 1-33, Inage-ku, Chiba 263-8522, Japan*
[b]*Osaka National Research Institute, AIST, Midoriga-oka, Ikeda, Osaka 563-8577, Japan*
[c]*Graduate School of Science and Technology, Kobe University, Rokkodai-cho 1-1, Nada-ku, Kobe 657-8501, Japan*
[d]*Department of Photonics, Faculty of Science and Engineering, Ritsumeikan University, Kusatsu, Siga 525-8577, Japan*
[e]*Graduate School of Science and Technology, Niigata University, Igarashi 2-no cho, Niigata 950-2102, Japan*
[f]*Japan Atomic Energy Research Institute, Tokai Establishment, Tokai-mura, Naka-gun, Ibaraki 319-1195, Japan*

Received 29 May 2000; accepted 4 June 2000

Abstract

The short-range structure of K_2O–$9TeO_2$ and K_2O–$4TeO_2$ in amorphous states such as glass and melt has been investigated by X-ray diffraction (XRD) and semi-empirical molecular orbital calculation (AM1-MOPAC method). The structure of amorphous alkali tellurites consisted of the TeO_4 trigonal bipyramids (tbp) and the TeO_3 trigonal pyramids (tp). Confirmed in the present work is that the TeO_4 trigonal bipyramids characteristics of TeO_2-based glasses transform into TeO_3 trigonal pyramids with increasing modifier K_2O content and a rise of temperature. The usage of XRD and MOPAC enabled us to comprehend in some details what to happen in phase transition from glasses to melts.

Keywords: Amorphous materials; X-ray diffraction

1. Introduction

There have been reported many studies of the tellurite glasses from scientific and technological points of view on account of their low melting temperatures [1,2], large thermal expansion [3], high dielectric constants [4], high refractive indexes, and good transmission for infrared lights with a wide range of wavelength [5]. Nowadays, these features of the tellurite glasses have been considered to promise for use as optical fiber or non-linear optical materials [6]. The structures of TeO_2-based glasses have frequently been examined by Raman and IR spectroscopy, reporting that there are two types of basic structural units such as TeO_4 trigonal bipyramid (tbp) with two equatorial and two axial Te–O bonds and a lone pair of electrons located on the third equatorial site, and TeO_3 trigonal pyramid (tp) [7]. In these structures, the coordination circumstance of Te changes from TeO_4 to TeO_3 with increasing alkali metal ions or a rise of temperature [8]. These spectroscopic measurements were, in fact, powerful tools for qualitative discussions of chemical species in glasses since it seemed easy to distinguish TeO_4 from TeO_3 in Raman and IR measurements, but unfortunately semi-quantitative for evaluation in the fractions of the structure units. On the contrary, X-ray diffraction provides one-dimensional interpretation of glass structures through the radial distribution function (RDF). Te–O and O–O distances and the coordination number of oxygen around tellurium are obtained with ease from RDF. The short-range structure of amorphous K_2O–TeO_2 was thus analyzed by X-ray diffraction in this study. Prior to the structural analysis of tellurite glasses, it is necessary to construct proper structural models for K_2O–TeO_2 glasses and melts. The semi-empirical molecular orbital calcula-

*Corresponding author. Tel.: +81-43-290-3433; fax: +81-43-290-3039.

E-mail address: iwadate@xtal.tf.chiba-u.ac.jp (Y. Iwadate).

0925-8388/00/$ – see front matter
PII: S0925-8388(00)01080-X

tion techniques called MOPAC was carried out to model glasses and to utilize the results as initial values in the structure optimization. The main purpose of this study is to examine the structure of alkali tellurite glasses and to demonstrate the usefulness of MO calculations in structural analysis of inorganic materials.

2. Experimental

Potassium tellurite glasses were prepared from the chemicals of reagent grade K_2CO_3 and TeO_2 so as to mix in prescribed ratios. The xK_2O–$(1-x)TeO_2$ ($x=0.1$ and 0.2) glasses and melts were prepared by a roller-quenching technique using a twin-roller apparatus with a thermal-image furnace [9,10]. Mixtures of these materials with appropriate compositions were melted at 973 and 1173 K for 1 h in a platinum crucible, respectively. The resultant melt was poured into rotating twin rollers (3000 rpm) to yield thin flakes. The quenching rate was estimated to be 10^5–10^6 K s^{-1}. The compositions were chemically analyzed to be unchanged within the experimental errors. The densities of glasses were taken from the literature [7], being estimated to be 5.461 g cm^{-3} for $x=0.1$ and 4.243 g cm^{-3} for $x=0.2$. The densities of melts were regarded to be almost equivalent to those of the corresponding glasses since the volume changes on melting were negligibly small in both systems. The conventional diffraction technique was employed in the measurements of glassy powders. But the melts were contained in a Pt vessel, the scattered X-ray from the surface of which was counted.

Scattered X-ray intensities were measured with an X-ray diffractometer (TTRAX type, Rigaku, Osaka) having a θ–θ type reflection geometry with an SSD (solid-state detector) using Mo Kα radiation with a continuous output of 60 kV and 300 mA. Measurements were made using a step-scanning technique for every 0.25°; in the low angle range of $2.5° \leqslant \theta \leqslant 15°$ and in the high angle range of $12.5° \leqslant \theta \leqslant 60°$, covering from 7.72 to 153.1 nm^{-1} in the magnitude of wave vector $Q=4\pi \sin\theta/\lambda$ where λ is the wavelength of the radiation, 0.07107 nm. Divergence and scattering slits of 0.5–0.5° and 1–1° were employed for the low angle region and high angle region, respectively. The receiving slit was 0.6 mm throughout this work. Accumulated intensities were combined smoothly by scaling the data in the overlapped θ region. The intensity data were corrected for background, polarization factor, absorption factor and Compton scattering by the usual method [11], and then normalized with the Krogh-Moe and Norman method [12,13] and the high-angle region method [14], so that the difference between normalization factors became less than 0.1% over the range $140.0 \leqslant Q \leqslant 153.1$ nm^{-1}. Atomic scattering factors and Compton scattering factors were taken from the literature [15,16].

3. Results and discussion

3.1. X-ray diffraction

The analytical functions used in this work are described briefly as follows. The interference function $Q \cdot i(Q)$, the radial distribution function $D(r)$ and the correlation function $G(r)$ are defined by Eqs. (1)–(3),

$$Q \cdot i(Q) = Q \cdot \left[I_{eu}^{coh}(Q) - \sum_i f_i(Q)^2 \right] / \left(\sum_i f_i(Q) \right)^2 \quad (1)$$

$$D(r) = 4\pi r^2 \rho_0 + (2r/\pi) \int_0^{Q_{max}} Q \cdot i(Q) \sin(Qr)\, dQ \quad (2)$$

$$G(r) = 1 + (2\pi^2 r \rho_0)^{-1} \times \int_0^{Q_{max}} Q \cdot i(Q) \sin(Qr)\, dQ \quad (3)$$

where Q is the wave vector defined before, $f_i(Q)$ the theoretical independent atomic scattering amplitude, ρ_0 the number of stoichiometric units per unit volume, $I_{eu}^{coh}(Q)$ the total coherent intensity function, Q_{max} the maximum value of Q reached in the scattering experiment. Summation is made over the stoichiometric units in a glass. Introduction of the term $(\Sigma f_i(Q))^2$ into Eq. (1) makes the product $f_i(Q)f_j(Q)/(\Sigma f_i(Q))^2$ in Eq. (4) nearly independent of Q and thus removes from the resulting correlation function most of the average breadth of the distribution of electron density in the atoms.

$$\begin{aligned} i(Q) &= \left[I_{eu}^{coh}(Q) - \sum_i f_i(Q)^2 \right] / \left(\sum_i f_i(Q) \right)^2 \\ &= \left[\sum_i \sum_j f_i(Q) f_j(Q) / \left(\sum_i f_i(Q) \right)^2 \right] \\ &\quad \times 4\pi r^2 \int_0^{\infty} [\rho_{ij}(r) - \rho_0] \sin(Qr)/(Qr)\, dr \end{aligned} \quad (4)$$

where the function $i(Q)$ is related to the radial density $4\pi r^2 \rho_{ij}(r)$ of distinct atoms pairs i–j. The analytical procedures were about the same as those of Narten [17].

It is necessary for the structural analysis of glass to understand what is the most basic short-range structure for the investigated glass. In case of alkali tellurite glasses, it has been proposed that two types of Te–O coordinations are presented, one is formed by the long Te–O bond ($\fallingdotseq$0.2 nm) and the other the short Te–O bond ($<$0.2 nm) [18]. Fig. 1 shows the radial distribution function $D(r)$ and the scaled function $D(r)/r$ of K_2O–$9TeO_2$ glass. The function $D(r)$ reveals the information of time and space averaged atomic arrangement, being one-dimensional interpretation of glass structures. In the $D(r)$, the near neighbor coordination number is usually evaluated from integration of the first peak area. The first peak in Fig. 1 was, however, not a Gaussian-type function probably due to the overlapping of

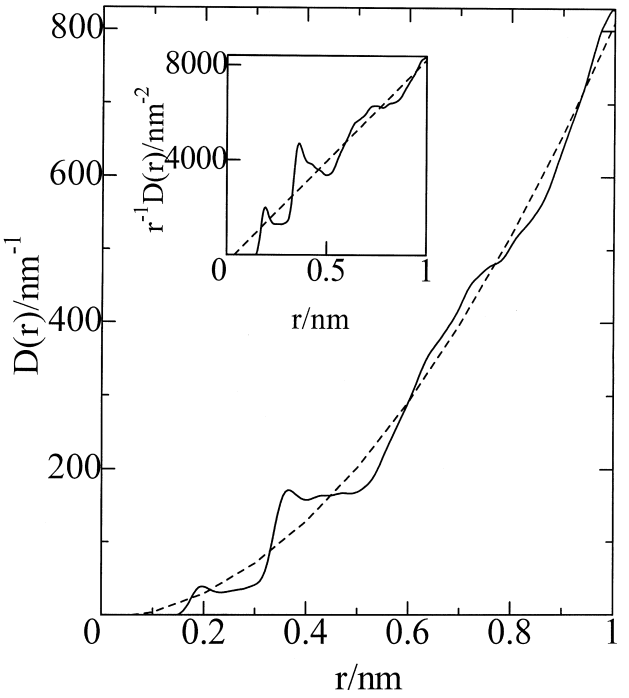

Fig. 1. Radial distribution function $D(r)$ and scaled function $D(r)/r$ of K_2O–$9TeO_2$ glass.

some peaks. The same tendency was observed at the other composition.

The correlation functions $G(r)$s in glassy and molten K_2O–TeO_2 systems are depicted in Fig. 2. There appeared two clear peaks at about 0.20 and 0.36 nm. Another small peak around 0.27 nm was observed in the profiles of three samples except for K_2O–$9TeO_2$ glass. The first peaks at around 0.20 nm were thought to be due to the nearest neighbor Te–O correlation by taking into account the ionic radii of Te^{4+}, K^+ and O^{2-} which were evaluated by Shannon [19] to be 0.056, 0.138 and 0.140 nm, respectively. However, some overlapping of the atomic pair correlations should be considered since the first peaks on $D(r)/r$ curve shown in Fig. 1 were asymmetric on the tail ends. The second small peak at about 0.27 nm was expected to be assigned to the O–O and K–O correlations. It might be assignable to the K–O correlation because the intensities of the first peaks at around 0.20 nm decreased and those of the second small peaks at about 0.27 nm increased with increasing K_2O content. The third peaks at around 0.36 nm in the correlation function $G(r)$ were thought to be attributed mainly to the Te–Te pair, and there were many other correlations after this distance because of the broad profiles in the peaks. As mentioned above, only information on the nearest neighbor can easily be obtained from $D(r)$ or $G(r)$ analysis, as was not the case with the other correlations.

In order to refine the short-range structure of the K_2O–TeO_2 glasses and melts, the structural parameters for each

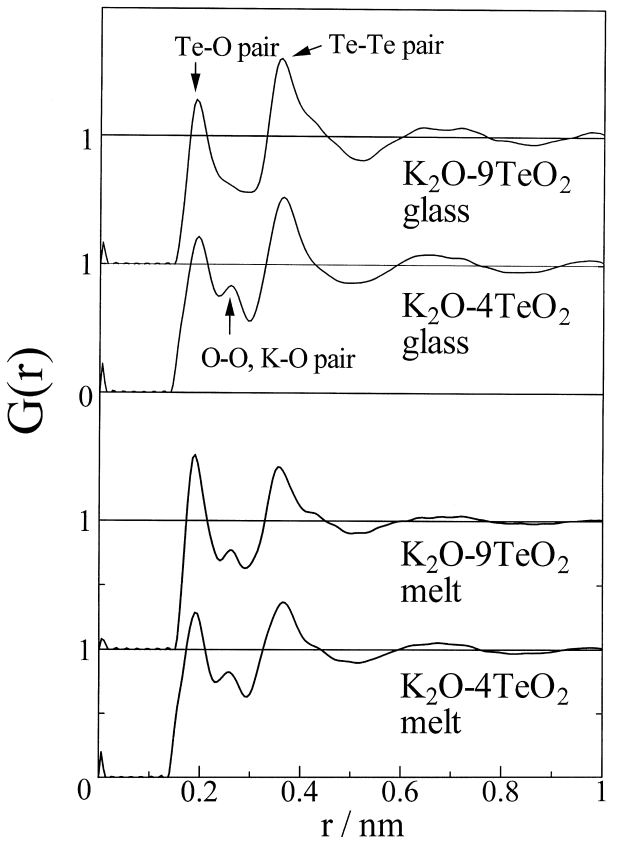

Fig. 2. Correlation function $G(r)$ of glassy and molten K_2O–TeO_2 systems.

atomic pair are needed to be optimized in $(Q, Q\cdot i(Q))$ space by the correlation method, using the non-linear least-squares fitting of Eq. (5) [17].

$$Q\cdot i(Q)=\left[\sum_i\sum_j n_{ij} f_i(Q) f_j(Q) \exp(-b_{ij}Q^2)\sin(Qr_{ij})/r_{ij}\right] \Big/ \left(\sum_i f_i(Q)\right)^2 \quad (5)$$

where n_{ij}, r_{ij}, and b_{ij} refer to the average coordination number, the average interatomic distance, and the temperature factor for the atomic pair i–j, respectively. Each atomic pair was presumed to be Gaussian distributed and centered at r_{ij} with a mean square displacement $2b_{ij}$. The initial values of the structural parameters were preset to be equal to those obtained in $D(r)$ or $G(r)$ analysis or taken from the crystallographic data of K_2O [20], considering the results of MOPAC described afterwards. The prescribed $Q\cdot i(Q)$ equation on the bases of the Debye scattering equation was applied to the model structure of the glass and melt, and the $Q\cdot i(Q)$ calculated from the model was compared with the observed $Q\cdot i(Q)$ in $(Q, Q\cdot i(Q))$ space [21,22]. The interference functions $Q\cdot i(Q)$s of glassy and molten K_2O–TeO_2 systems are illustrated in Fig. 3. The calculated $Q\cdot i(Q)$ revealed a good agreement with the

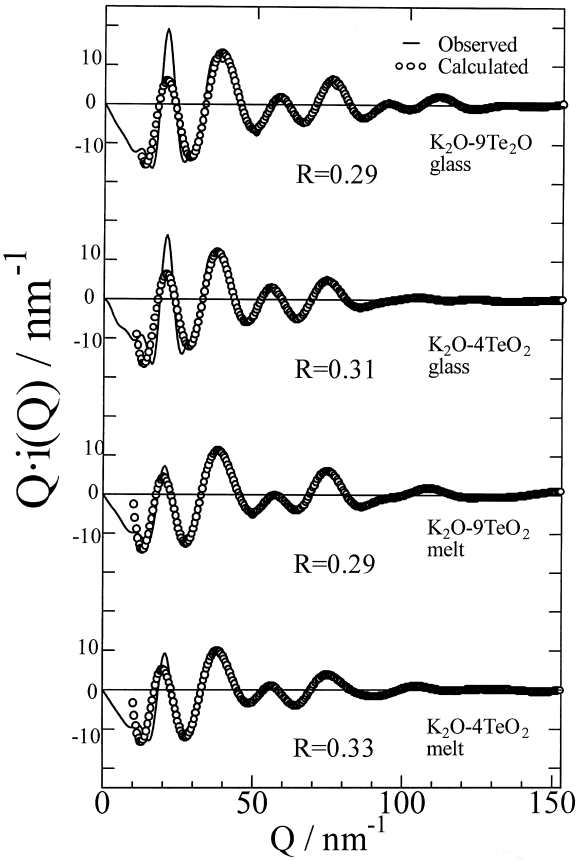

Fig. 3. Interference function $Q \cdot i(Q)$ of glassy and molten K_2O–TeO_2 systems.

observed $Q \cdot i(Q)$ in the Q-range of more than 10 nm^{-1}. The degree of coincidence in fitting, R, defined by Eq. (6),

$$R = \sum |Q \cdot i(Q)_{obs} - Q \cdot i(Q)_{calc}| / \sum |Q \cdot i(Q)_{obs}| \quad (6)$$

were estimated at around 0.3, indicating that the obtained structural parameters reproduced the real structure of glasses and melts with a fairly accuracy. The least-squares fitted structural parameters are listed in Tables 1 and 2, where the statistical errors in n_{ij}, r_{ij}, b_{ij}, and $\langle \Delta r_{ij}^2 \rangle^{1/2}$ were estimated at ± 0.2, ± 0.001 nm, $\pm 0.5 \times 10^{-6}$ nm^2, and ± 0.001 nm, respectively. As described before, there were two types of near neighbor Te–O distances, i.e., one was at around 0.18 nm and the other around 0.20 nm. This trend was consistent with those of the other alkali tellurite glasses having two sorts of Te–O pairs in the TeO_4 trigonal bipyramids (tbp) [3]. As can be seen in Tables 1 and 2, the third Te–O pair was observed at about 0.24 nm. This would be due to the fact that the Te–O bonds in the TeO_4 trigonal bipyramids (tbp) were broken partly into TeO_3 trigonal pyramids with increasing K_2O and a rise of temperature (phase change). The total coordination number of O around Te (in the first coordination shell) decreased with increasing K_2O content and a rise of temperature. The results suggest that the alkali tellurite glasses having lower K_2O content had networks composed of mainly TeO_4 trigonal bipyramids (tbp). Actually, Yoko et al. have pointed out that TeO_4 trigonal bipyramids (tbp) convert to TeO_3 trigonal pyramids (tb) and pass by the TeO_{3+1} polyhedra having non-bridging oxygen [23] by the addition of K_2O content and with the increase of temperature.

It should be noted that the contributions of O–O and K–O pair correlations to the $D(r)$ or $G(r)$ curve were rather difficult to be estimated since the compositional ratios of K to O or Te were very small and the atomic scattering factor of Te was rather greater than those of O and K. Consequently, the peaks of O–O and K–O pairs were in effect undetectable in the $D(r)$ or $G(r)$ curve. In this work, the initial values of the K–O distance and the coordination number of O around K were preset for 0.27 nm considering the ionic radii and 6 on the basis of the crystallographic data [20], respectively, and the other structural parameters were refined.

Akagi et al. have carried out an XAFS spectroscopy and high-temperature Raman spectroscopy for K_2O–TeO_2 glasses and melts [24], determining that the potassium tellurite glasses consist of both TeO_4 trigonal bipyramids and TeO_3 trigonal pyramids, and TeO_4 trigonal bipyramids convert to TeO_3 trigonal pyramids by the addition of K_2O and with an increase of temperature. It was also found that the K–O distances were almost equal to the sum of the ionic radii K^+ and O^{2-} (=0.276 nm), and that total coordination number of oxygen atoms around potassium

Table 1
Least-squares fitted structural parameters of K_2O–$9TeO_2$ glass and melt

ik	Glass				Melt			
	n_{ik}	r_{ik} (nm)	b_{ik} (nm^2)	$\langle \Delta r_{ij}^2 \rangle^{1/2}$ (nm)	n_{ik}	r_{ik} (nm)	b_{ik} (nm^2)	$\langle \Delta r_{ij}^2 \rangle^{1/2}$ (nm)
Te–O	1.53	0.180	2.68E-5	7.32E-3	1.52	0.181	3.14E-5	7.92E-3
Te–O	1.96	0.205	3.64E-5	8.53E-3	1.86	0.204	5.24E-5	1.02E-2
Te–O	0.97	0.239	5.16E-5	1.06E-2	0.81	0.248	7.85E-5	1.25E-2
O–O	4.23	0.260	6.04E-5	1.10E-2	3.88	0.261	9.03E-5	1.34E-2
O–O	3.42	0.277	6.23E-5	1.12E-2	3.52	0.276	9.90E-5	1.41E-2
K–O	7.01	0.292	7.60E-5	1.23E-2	6.99	0.283	1.20E-4	1.55E-2
Te–Te	2.28	0.355	2.32E-4	2.16E-2	2.02	0.353	2.70E-4	2.32E-2
Te–Te	3.08	0.406	9.74E-4	4.41E-2	3.00	0.411	1.01E-3	4.50E-2

Table 2
Least-squares fitted structural parameters of K_2O–$4TeO_2$ glass and melt

ik	Glass				Melt			
	n_{ik}	r_{ik} (nm)	b_{ik} (nm^2)	$\langle \Delta r_{ij}^2 \rangle^{1/2}$ (nm)	n_{ik}	r_{ik} (nm)	b_{ik} (nm^2)	$\langle \Delta r_{ij}^2 \rangle^{1/2}$ (nm)
Te–O	1.10	0.176	4.39E-5	9.37E-3	1.49	0.177	6.04E-5	1.10E-2
Te–O	2.00	0.202	6.98E-5	1.18E-2	1.69	0.202	6.34E-5	1.13E-2
Te–O	1.04	0.239	7.73E-5	1.24E-2	0.82	0.241	7.88E-5	1.26E-2
O–O	4.13	0.264	8.05E-5	1.27E-2	4.13	0.264	8.50E-5	1.30E-2
O–O	3.75	0.269	8.30E-5	1.29E-2	3.01	0.266	9.48E-5	1.38E-2
K–O	5.89	0.271	8.52E-5	1.31E-2	5.24	0.267	2.89E-4	2.40E-2
Te–Te	2.98	0.359	3.71E-5	2.72E-2	2.83	0.356	4.58E-4	3.03E-2
Te–Te	2.46	0.405	9.85E-4	4.44E-2	2.48	0.414	10.3E-4	4.54E-2

was almost 6. As can be seen from the K–O correlations in Tables 1 and 2, the coordination number decreased on the phase change from glass to melt as usual. The coordination number of O atom around K atom in both glass and melt of K_2O–$9TeO_2$ composition was estimated at about 7 and that of K_2O–$4TeO_2$ composition from 5.2 to 5.9. The K–O distance in K_2O–$9TeO_2$ composition was calculated to be 0.283–0.292 nm, that in K_2O–$4TeO_2$ composition being 0.267–0.271 nm. This slight difference in composition of K_2O leads to the marked decreases in the coordination number and the interatomic distance for K–O pair. These findings might indicate that the bond nature between K and O was not covalent but ionic, and thus the potassium atoms distributed easily and unrestrictedly as K^+ ions in the gaps of network formed by TeO_3 or TeO_4 structural units. The XAFS spectroscopy [24] also revealed that potassium ions had a similar local structure in all K_2O–TeO_2 glasses studied. Not only the present work but also the Raman spectra [24] supported the model described before, such that the network forming Te–O bonds has been broken and a part of TeO_4 trigonal bipyramids have changed into TeO_3 trigonal pyramids by the addition of K_2O and with an increase of temperature.

3.2. MOPAC

The semi-empirical molecular orbital calculation (AM1-MOPAC) was applied to confirm the results given as the structural parameters through XRD in this work, XAFS and Raman spectroscopy [24]. In the molecular orbital calculations the MOPAC97 program (winMOPAC) installed on the Windows 95 machine was used [25]. As mentioned before, alkali tellurite glasses consisted of two types of network forming units, the TeO_4 trigonal bipyramids (tbp) and the TeO_3 trigonal pyramids (tb). Calculations were made until the model structure was in the most stabilized state energy, which has the geometry optimized structure, and were finally adopted to the calculation of the $Te_3O_{10}^{4-}$ which is supposed to be the most basic model-network structure in alkali tellurite glass (tellurite-rich) after computations of several models. The geometrically optimized structure $Te_3O_{10}^{4-}$ is illustrated in Fig. 4 and the numerical results tabulated in Table 3. Two types of Te–O bond lengths exist with certainty, as listed in Table 3. The bond lengths of Te–Te were also in fair agreement with the experimental structural data (0.36 nm), although the calculated bond lengths are a little different from the experimental ones. MOPAC calculations are thought to reproduce in some extent the short-range structure of alkali tellurite glasses and melts.

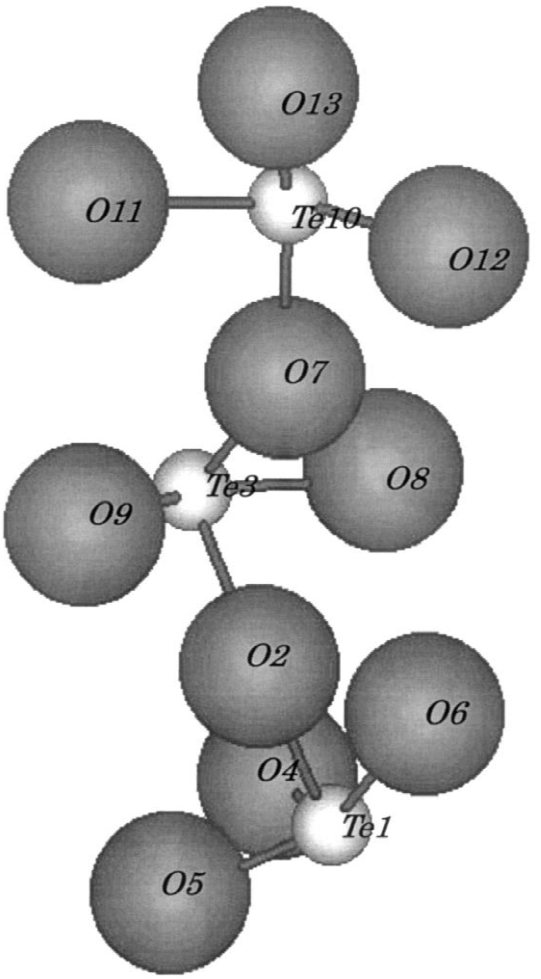

Fig. 4. Geometry optimized structure of $Te_3O_{10}^{4-}$ by AM1-MOPAC calculation.

Table 3
Geometry optimized parameter of $Te_3O_{10}^{4-}$ by AM1-MOPAC calculation

Atomic pair	Bond length (nm)	Atomic pair	Bond length (nm)
TE3–O2	0.188	O2–O7	0.293
TE3–O7	0.189	O2–O8	0.241
TE3–O8	0.195	O2–O9	0.240
TE3–O9	0.194	TE1–TE3	0.354
–	–	TE3–TE10	0.320

4. Conclusion

According to X-ray diffraction (XRD) and semi-empirical molecular orbital calculation (AM1-MOPAC method), the short-range structure of K_2O–TeO_2 systems in amorphous states such as glass and melt has been investigated. The results obtained in the present work is that the structure of amorphous potassium tellurite consisted of the TeO_4 trigonal bipyramids (tbp) and the TeO_3 trigonal pyramids (tp), and the TeO_4 trigonal bipyramids convert to TeO_3 trigonal pyramids with increasing modifier K_2O content and a rise in temperature. In the TeO_4 trigonal bipyramids (tbp), there are two sorts of near neighbor Te–O distances. The shorter is at around 0.18 nm and the longer is at around 0.20 nm. These finding were semi-quantitatively interpreted by the MOPAC calculations.

Acknowledgements

The present work has been carried out as a part of the JAERI-University Research Cooperation financially and technically supported by the Inter-University Program for the Joint Use of JAERI Facilities and owing to the Regulations for Acceptance of Guest Research by AIST Institutes.

References

[1] J.E. Stanworth, J. Soc. Glass Technol. 36 (1952) 217.
[2] J.E. Stanworth, J. Soc. Glass Technol. 38 (1954) 425.
[3] K. Tanaka, T. Yoko, H. Yamada, J. Kamiyama, J. Non-Cryst. Solids 103 (1988) 250.
[4] J.E. Stanworth, Nature 169 (1952) 581.
[5] H. Burger, W. Vogel, V. Kozhukharov, Infrared Phys. 25 (1985) 395.
[6] M. Tatsumisago, T. Minami, Ceramics 28 (1993) 1227.
[7] T. Sekiya, N. Mochida, A. Ohtsuka, M. Tomokawa, J. Non-Cryst. Solids 144 (1992) 128.
[8] Y. Kowada, K. Habu, H. Adachi, Chem. Express 7 (1992) 965.
[9] M. Tatsumisago, T. Minami, M. Tanaka, J. Am. Ceram. Soc. 64 (1981) C97.
[10] M. Tatsumisago, T. Minami, Y. Kowada, H. Adachi, Phys. Chem. Glasses 35 (1994) 89.
[11] H.A. Levy, M.D. Danford, A.H. Narten, ORNL-3960, Oak Ridge National Laboratory report, USA, 1966.
[12] J. Krogh-Moe, Acta Crystallogr. 9 (1956) 951.
[13] N. Norman, Acta Crystallogr. 10 (1957) 370.
[14] H. Ohno, K. Furukawa, Met. Phys. Semin. 3 (1978) 129.
[15] J.A. Ibers, W.C. Hamilton (Eds.), International Tables for X-ray Crystallography, Vol. 4, Kynoch, Birmingham, 1974, p. 99.
[16] F. Hajdu, Acta Crystallogr. Sect. A27 (1971) 73.
[17] A.H. Narten, J. Chem. Phys. 56–5 (1972) 1905.
[18] K. Tanaka, T. Yoko, H. Yamada, K. Kamiya, J. Non-Cryst. Solids 103 (1988) 1905.
[19] R.D. Shanon, Acta. Crystallogr. A32 (1976) 751.
[20] R.W.G. Wyckoff, in: Crystal Structures, Vol. 1, Interscience, New York, 1965, p. 240.
[21] H. Morikawa, F. Marumo, T. Koyama, M. Yamane, A. Oyobe, J. Non-Cryst. Solids 56 (1983) 355.
[22] Y. Iwadate, K. Igarashi, T. Hattori, S. Nishiyama, K. Fukushima, J. Mochinaga, N. Igawa, H. Ohno, J. Chem. Phys. 99 (1993) 6890.
[23] T. Yoko, K. Kamiya, K. Tanaka, H. Yamada, S. Sakka, J. Ceram. Soc. Jpn. 97 (1989) 289.
[24] R. Akagi, K. Handa, N. Ohtori, A.C. Hannon, M. Tatsumisago, N. Umesaki, Jpn. J. Appl. Phys. 38 (Suppl. 1) (1999) 160.
[25] J.J.P. Stewart, MOPAC 97 Fujitsu Limited, Tokyo, Japan, 1998.